

Development of a New Piezoelectrically Actuated Micropump for Liquid and Gas

Chiang-Ho Cheng, An-Shik Yang, Chih-Jer Lin, Chun-Ying Lee

Abstract—This paper aims to present the design, fabrication and test of a novel piezoelectric actuated, check-valves embedded micropump having the advantages of miniature size, light weight and low power consumption. This device is designed to pump gases and liquids with the capability of performing the self-priming and bubble-tolerant work mode by maximizing the stroke volume of the membrane as well as the compression ratio via minimization of the dead volume of the micropump chamber and channel. By experiment apparatus setup, we can get the real-time values of the flow rate of micropump, the displacement of the piezoelectric actuator and the deformation of the check valve, simultaneously. The micropump with check valve 0.4 mm in thickness obtained higher output performance under the sinusoidal waveform of 120 V_{pp}. The micropump achieved the maximum pumping rates of 42.2 ml/min and back pressure of 14.0 kPa at the corresponding frequency of 28 and 20 Hz. The presented micropump is able to pump gases with a pumping rate of 196 ml/min at operating frequencies of 280 Hz under the sinusoidal waveform of 120 V_{pp}.

Keywords—Actuator, Check-valve, Micropump, Piezoelectric.

I. INTRODUCTION

MICRO-fluidic system has been one of the most intensive research areas for micro-electro-mechanical systems (MEMS) over the past two decades. A variety of micro-fluidic devices can be extensively applied to the fields of chemical analysis, drug delivery, life science, molecular separation and precise flow control systems. Micropumps are essential components of micro-fluidic systems for handling precise volumes of liquid in the applications such as delivery in drug, fuel cells, ink jet printers, and bio-fluidics. To develop miniature devices which can pump, mix, sense, and control a minute amount of fluid, a micro-fluidic system based on MEMS technologies is an immediate solution to achieve this purpose. The advantages of MEMS micropumps are due to their small-size, light weight, and cost reduction. In addition, the technological development has been pushed toward lab-on-chip (LOC) methodologies, where a micropump is used

to deliver a small amount of liquid precisely in a large integrated system.

As a result, micropumps have been an important topic for many researches as presented in several excellent reviewed papers discussing about the types of micropumps, theory and principle of micropumps, valve design, actuation methods, materials and fabrication technologies, and microfluidic manipulation [1]-[6]. The actuation forms can be divided into two categories: mechanical and non-mechanical actuation in general. Since there are no moving elements, the structure of non-mechanical micropumps is simpler than that of mechanical micropumps. Mechanical micropumps are relatively less sensitive to the liquid properties as compared to those non-mechanical micropumps. Mechanical micropumps can be further classified into two categories according to valve types, which are valveless micropumps [7], [8] and check valve micropumps [9], [10]. The structures of the valveless micropumps are relatively simple; therefore, they are easy to be fabricated. However, the issues of backflow and random flow are not evitable for the valveless micropumps. In contrast, the check valve micropumps show better performance to manage the backflow and random flow problems; though the fabrication processes of most check valve micropumps are more challenging and complex in general.

The operating pressures of polymers-made check valves are substantially lower than those made of silicon and metal because of small Young's modulus values of polymers materials as compared to those of silicon and metal. A softer polymeric material also offers much better sealing characteristics. Several works on polymeric check valves was presented, such as check valves were fabricated in polyimide [11], [12], polyester [13], parylene [9], silicone rubber [14], SU-8 [15] and PDMS [16]. The PDMS has good processing and sealing properties with a comparatively lower Young's modulus value than other polymers. Accordingly, PDMS was used to fabricate the check valves in this study.

Some earlier reported micropumps are lack of a self-priming feature with quite large dead and small stroke volumes. Their tests usually required complex preparation procedures for filling liquid and exhaust air bubbles. Therefore, this research aims to describe the design, fabrication and test of a novel micropump with cantilever check valves. The proposed novel design of micropump has large volume stroke ratio, which is defined as the stroke volume divided by the total chamber volume. The proposed micropump is mainly designed to pump gas and liquid with maximizing the stroke volume of the membrane.

Chiang-Ho Cheng is with the Department of Mechanical and Automation Engineering, Da-Yeh University, Changhua, 515, Taiwan (phone: (886) 4-8511888 ext. 2119; e-mail: chcheng@mail.dyu.edu.tw).

An-Shik Yang is with the Department of Energy and Refrigerating Air-Conditioning Engineering, National Taipei University of Technology, Taipei, 106, Taiwan (e-mail: asyang@ntut.edu.tw).

Chih-Jer Lin is with the Institute of Automation Engineering, National Taipei University of Technology, Taipei 106, Taiwan. (e-mail: cjlin@ntut.edu.tw).

Chun-Ying Lee is with the Department of Mechanical Engineering, National Taipei University of Technology, Taipei 10608, Taiwan (e-mail: leech@ntut.edu.tw).

II. DESIGN

Fig. 1 shows a novel micropump with check valve proposed in this study and its top view and the cross-section view of the structure on the AA section are shown in Figs. 2 and 3, respectively. The micropump consists of several structural layers from bottom up: an acrylic substrate as the lower cover, a piezoelectric disc as the actuator, a thin flexible membrane as the chamber layer to define the actuation area, an acrylic channel layer with a channel to introduce the driving pressure, two PDMS cantilever valve and stoppers used to open or close the channel, and an acrylic substrate as the top cover to form the channel with the channel plate.

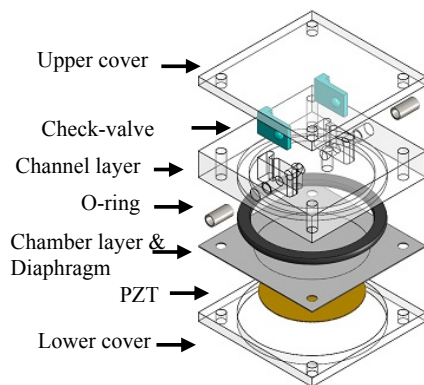


Fig. 1 Schematic of the micropump with check valves

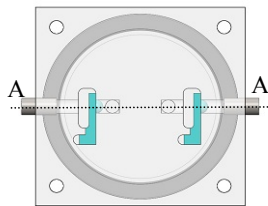


Fig. 2 The top view of the micropump

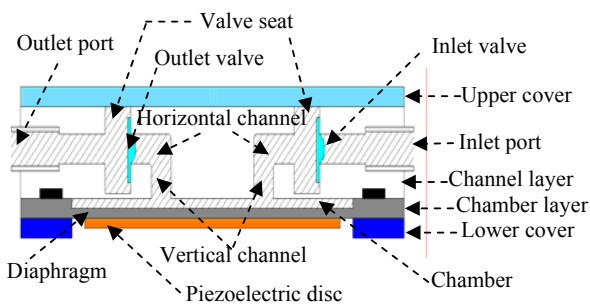


Fig. 3 The AA section view for the micropump

During operations, the piezoelectric is first actuated by the positive voltage to direct the diaphragm away from the chamber causing a decrease of chamber pressure due to the volume enlargement. Then, the inlet valve opens with closing of the outlet valve, and the liquid or air is sucked into the chamber from the inlet port. Afterward, the piezoelectric is actuated by

the negative voltage to make the diaphragm driven towards the chamber causing the volume shrinkage and the chamber pressure climb; thus, the inlet valve closes and the outlet valve opens with the liquid or air squeezed out of the chamber via the outlet port. As the piezoelectric is actuated periodically, the pumping medium is thus delivered from the inlet port to the outlet port continuously.

III. FABRICATION

A. Chamber Layer

The chamber layer was made of stainless steel substrate ($30 \text{ mm} \times 30 \text{ mm} \times 0.15 \text{ mm}$ in length, width and depth), which was fabricated by the MEMS-based lithography and wet etching process to form a circular cavity as the micropump chamber. The vibration diaphragm was made of the stainless steel substrate left after the wet etching process. The depth of chamber is $80 \mu\text{m}$ with the radius of 11 mm . An etchant consisting of 46g ferric chloride, 33g hydrogen peroxide and 54g deionized water was utilized to obtain smooth uniform channels on the stainless steel substrates. At the start, the AZ 9260 photoresist was coated on the stainless-steel substrate by spin coater with both spreading step and thinning step. The photoresist on the substrate was baked on a hot plate or in an oven, and then exposed by a standard UV mask aligner (Karl Suss MA-6). The UV exposure process was performed under the hard contact mode with an intensity of 6 mW cm^{-2} at a wavelength of 365 nm . The exposed photoresist was then developed in an immersion process via AZ400K diluted developer. Finally, the samples that were wet etched were immersed in the etchant at $53\text{--}58^\circ\text{C}$. The fabricated chamber layer is shown in Fig. 4.

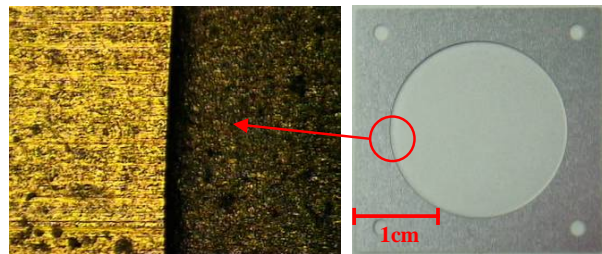


Fig. 4 The fabricated stainless steel chamber layer

B. Piezoelectric Actuator

The piezoelectric disc with $20 \text{ mm} \times 150 \mu\text{m}$ in diameter and thickness was prepared by the commercial available piezoelectric powder (ARIOSE Company, B6 type) through the dry powder pressing technique. The sintering process was performed in a tube furnace under a quiescent air atmosphere at a heating rate of 90°C/min to the peak temperatures of 1250°C for maintaining a duration of 2 hours, which followed by a 90°C/min cooling rate to the room temperature. The poling electrodes were patterned using a screen-printing technique with silver paste. For poling the piezoelectric, the poling electric field was $2.0 \text{ V}/\mu\text{m}$ under the temperature of 100°C in 15 minutes. As shown in Fig. 5, the P-E hysteresis curves were

measured by a high voltage test system (Radiant Technologies: Precision LC with HVI 10 kV). The coercive field (E_c) was 7.14 kV/cm; the saturated polarization (P_s) and remnant polarization (P_r) were $40.08 \mu\text{C}/\text{cm}^2$ and $33.93 \mu\text{C}/\text{cm}^2$, respectively. Fig. 6 shows the measurement results for the d_{33} characteristics of the piezoelectric discs, the average value of d_{33} are 512.0 pm/V with standard deviation of 2.738.

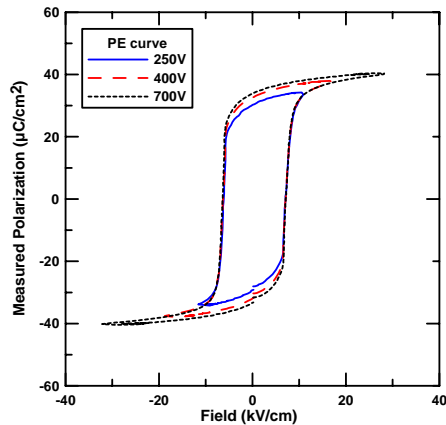


Fig. 5 P - E hysteresis curves of the Piezoelectric disc

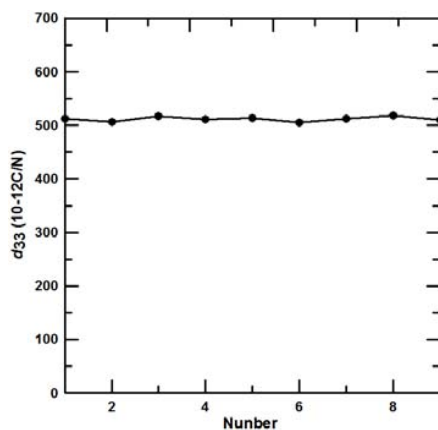


Fig. 6 d_{33} characteristics of the piezoelectric disc

C. Channel Layer

The channel layer was made of acrylic fabricated with the conventional CNC cutting and milling techniques. The acrylic plate was severed into the desired sizes ($30\text{mm} \times 30\text{mm} \times 5\text{mm}$ in length, width and height) and micro-milled to form two valve seats, two vertical channels and two horizontal channels for the inlet and outlet. The diameters of the horizontal and vertical flow channels are both 2mm, but their lengths are 1.25mm and 4mm, respectively.

D. Check Valve

The check valves were molded via a PDMS mixture. A 10:1 mixture of solution A and B supplied was stirred and degassed under the room temperature until the mixture became fully clear and bubble free. The solutions A and B work as the main agent and the coagulant, while the heating process can speed up

solidification. Hence, the prepared PDMS mixture was poured onto the check valve's mold and cured at 75°C for 2 h. After cooling, the products were taken out of the mould with great care so as to prevent damage to these very small and thin PDMS devices. The front and side views of check valve are shown in Fig. 7.

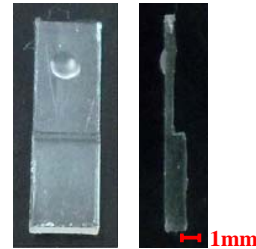


Fig. 7 Front and side view of check valve

E. Assembly

The first step of assembly was to pinpoint the o-ring and check valves on the channel layer. Then, the epoxy adhesive (3M, DP-460) was applied on the attached surfaces by screen printing to assemble the chamber layer and piezoelectric actuator by the aligned marks in conjunction with a CCD aligning system. The adhesive was cured in the oven kept at 60°C for 2 hours to prevent from depolarization. Finally, the stack of these four layers (Upper cover, Channel layer, Chamber layer, Lower cover) was fixed with four screws. The assembled device is shown in Fig. 8.

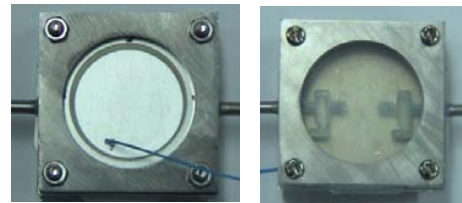


Fig. 8 The top and bottom view of assembled micropump

IV. EXPERIMENTAL APPARATUS

To understand the relation between the liquid flow rate and the actuator displacement of the micropump, we use the scanning laser vibrometer (Polytec MSV300) to measure the displacement and velocity of the piezoelectric actuator at the same time when the micropump is actuated at different operating frequency. Each datum obtained is the average value from three measured samples with the same conditions. The deviations of the three measured values from the average must be within 5%. Fig. 9 shows the schematic and the photograph of the experimental setup for the performance test of micropump. The function generator (Agilent 33120A) generates the driving signal, which is amplified by the voltage amplifier (Trek Model 601C) to actuate the piezoelectric actuator. The micropump is actuated to work and the electrical balance with the precision of 0.01 g is used to measure the liquid flow rate. The real-time measurement system designed by a LabView software interface

via the RS232 port is used to record the time history of flow rate.

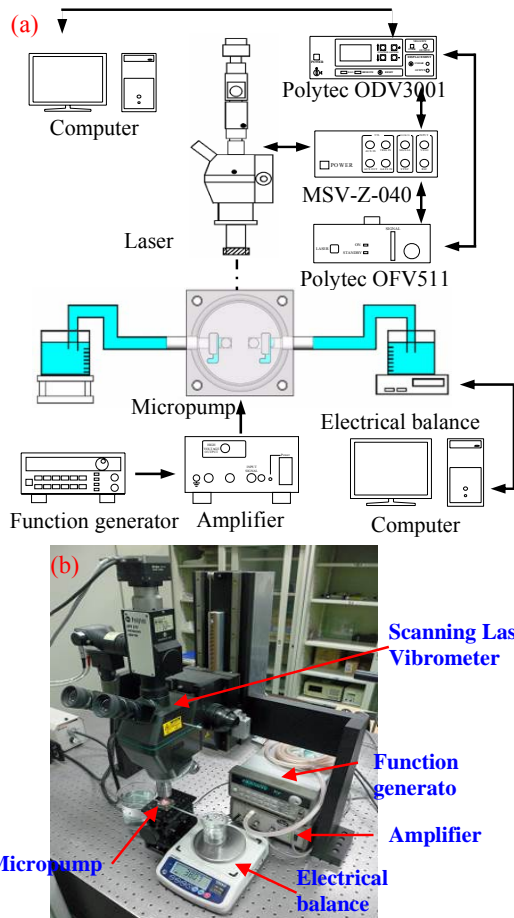


Fig. 9 (a) Schematic diagram and (b) photograph of the experimental setup for the performance test of micropump

V. PERFORMANCE OF MICROPUMP

A. Self-priming and Bubble-tolerant Test

Without pre-filling any liquid into the outlet and inlet ports of the micropump, the device was able to automatically suck water from the beaker and then pump the liquid from the inlet tube to the outlet tube for realizing its self-priming feature, under the operating conditions applying a peak-to-peak sine-wave voltage of 120 V in the range of 10-30 Hz to the piezoelectric disc. The photograph of the self-priming experimental is illustrated in Fig. 10 (a). To investigate the bubble-tolerant, the micropump was pre-filling water as the liquid with a small amount of bubbles attached to the connection soft tube between the outlet and inlet ports, as shown in Fig. 10 (b). The micropump tended to tolerate the presence of the air bubbles and release those bubbles out of the chamber without deteriorating the pumping performance.

B. Performance Characterization of Water

The micropump was tested with DI water and driven with

120 Vpp. The frequency dependence of the pumping rate at zero back pressure is shown in Fig. 11 for three different check valve thicknesses (0.3, 0.4 and 0.5mm). The maximum pumping rates of 36.8, 42.2 and 38.0 ml/min, respectively, were achieved at the frequency of 28 Hz. For the check valve with 0.3mm thick, the flow rate increased with the frequency and the first peak was at 28Hz; the flow rate decreased as the frequency beyond 28 Hz and it reached the minimum at 70Hz. After that, the flow rate increased again and reached the second peak at 150Hz; the flow rate then reduced with the frequency. The similar phenomenon occurred to the check valves with the thicknesses of 0.4 and 0.5mm. For the check valve with 0.4mm thick, the minimum was at 80 Hz and the second peak was at 160 Hz, while the first and second peaks were at 90 and 170 Hz respectively for the check valve with 0.5mm thick.

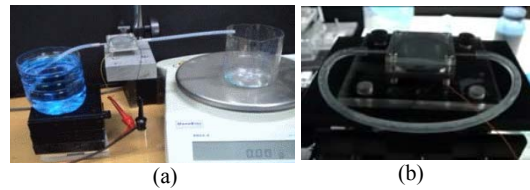


Fig. 10 (a) self-priming and (b) bubble-tolerant test of micropump

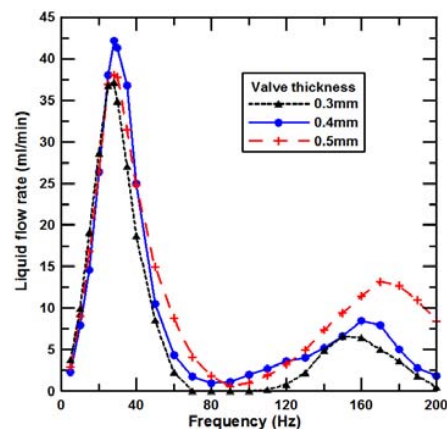


Fig. 11 Measured water flow rate versus operating frequency for three different check valve thicknesses

Figs. 12-14 show the relation between flow rate, velocity and displacement of the piezoelectric center for the check valve with the thickness of 0.3, 0.4 and 0.5 mm. From resulting experiments, the micropump with the different check valves all have the similar the relation between flow rate, velocity and displacement. That is, the flow rate is proportion to the velocity and displacement. The flow rate is the bigger as the piezoelectric actuator produces the larger displacement and velocity. Fig. 15 shows the relation between the frequency and the backpressure for three different check valves with different thicknesses. There are three peaks of backpressure for all three different check valves, whose thickness are 0.3, 0.4 and 0.5mm. The first peak is at 20 Hz and the maximal backpressure of 14.0kPa produced by the check valve with thickness of 0.4 mm. On the second peak, whose frequency is 60Hz, the check valve

with thickness of 0.5mm has the maximal backpressure. On the third peak, whose frequencies are 160, 170 and 180 Hz for the check valve with the thickness of 0.3, 0.4 and 0.5 mm, respectively. For the third peak, the thicker check valve has the larger frequency for the maximal backpressure.

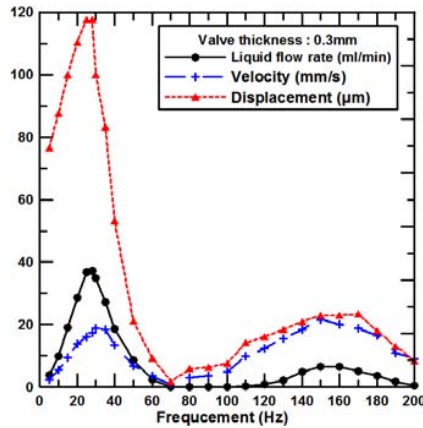


Fig. 12 The relation between the water flow rate, displacement and velocity for the check valve of 0.3 mm

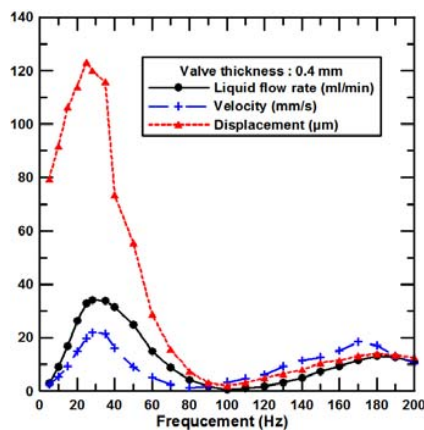


Fig. 13 The relation between the water flow rate, displacement and velocity for the check valve of 0.4 mm

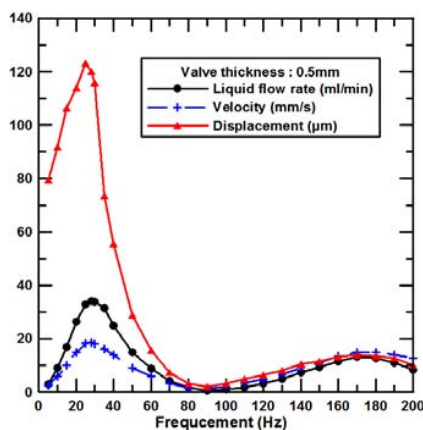


Fig. 14 The relation between the water flow rate, displacement and velocity for the check valve of 0.5 mm

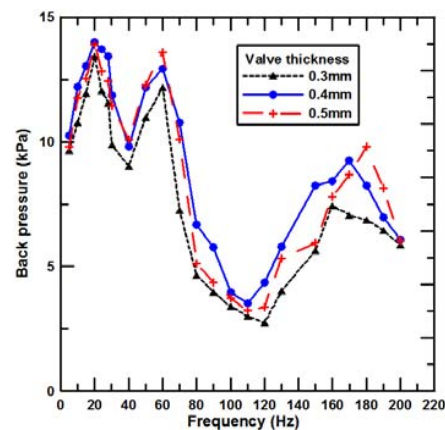


Fig. 15 Measured back pressure versus operating frequency for three different check valve thicknesses

In addition, the backpressure also affects the flow-rate of the micro-pump. Fig. 16 shows the relation between the flow-rate and the backpressure at a peak-to-peak sine-wave voltage of 120 V on the operation frequency of 28 Hz, where the micropump have the maximal flow-rates. As shown in Fig. 16, the check valve with the thickness of 0.4 (mm) has the maximal flow-rate of 42.2 ml/min at the maximal backpressure of 13.4kPa. On one hand, the flow-rate will decrease as the outer pressure and the inner pressure of the micropump reach a specified critical value; on the other hand, the flow-rate will converge zero as the micropump has the balance of the outer and inner pressure.

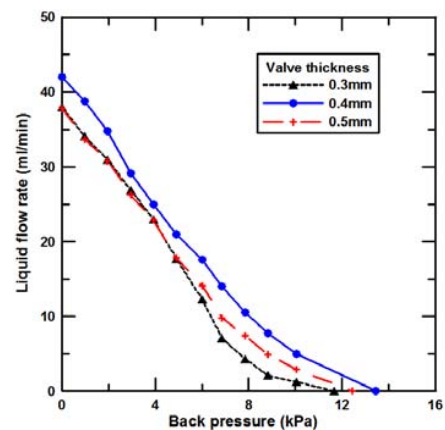


Fig. 16 Measured water flow rate versus back pressure for three different check valve thicknesses

C. Performance Characterization of Air

The special characteristic for the micropump is that it can also pump the air instead of the fluid; therefore, we should discuss the performance of the micropump for the air flow. The pump was tested with air and driven at 120 Vpp. The frequency dependence of the pump rate is shown in Fig. 17 for three different check valve thicknesses (0.3, 0.4 and 0.5mm). A maximum pump rate of 175, 196 and 182 ml/min, respectively,

was achieved at the frequency of 280 Hz. For the thickness of all check valves, the flow rate increased with the frequency and the maximum pump rate was at 280 Hz; the flow rate decreased at the frequency above 280 Hz. Fig. 18 shows that displacement of the piezoelectric center at all the operating frequencies for three different check valve thicknesses. When the actuation frequency was swept from 10 Hz to about 300 Hz, the displacement of piezoelectric actuator almost did not change with the actuation frequency.

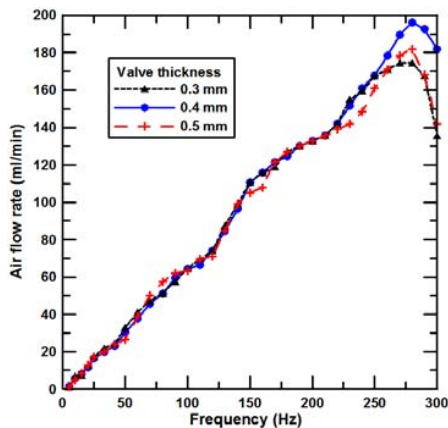


Fig. 17 Measured air flow rate versus operating frequency for three different check valve thicknesses

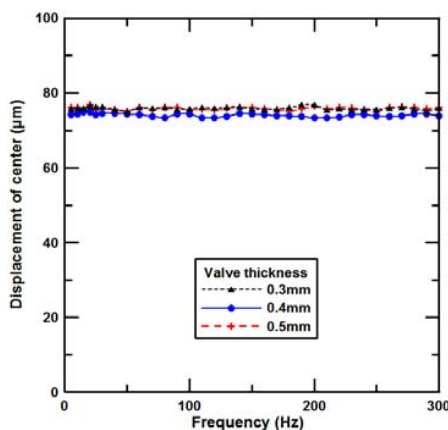


Fig. 18 The displacement of the piezoelectric center with respect to the frequency

VI. CONCLUSION

This paper described the design, fabrication and test of a check-valve embedded micropump for pumping gas and liquid. The micropump is designed to pump gases and liquids with the capability of performing the self-priming and bubble-tolerant work mode by maximizing the stroke volume of the membrane as well as the compression ratio via minimization of the dead volume of the micropump chamber and channel. The micropump with check valve 0.4 mm in thickness obtained higher output performance under the sinusoidal waveform of 120 Vpp. The micropump achieved the maximum pumping rates of 42.2 ml/min and back pressure of 14.0 kPa at the

corresponding frequency of 28 and 20 Hz. The presented micropump is able to pump gases with a pumping rate of 196 ml/min at operating frequencies of 280 Hz.

ACKNOWLEDGMENT

The authors would like to thank the National Science Council of the Republic of China, Taiwan for financially supporting this research under Contract No. NSC101-2221-E-212-002- and NSC102-2221-E-212-008-.

REFERENCES

- [1] N T Nguyen, X Huang and T K Chuan, "MEMS-micropumps: a review," *ASME J. Fluids Eng.* Vol. 124, pp. 384-392, 2002.
- [2] D J Laser and J G Santiago, "A review of micropumps," *J. Micromech. Microeng.* Vol. 14, pp. R35-R64, 2004.
- [3] P Woias, "Micropumps-past, progress and future prospects," *Sensors Actuators B* Vol. 105, pp. 28-38, 2005.
- [4] N C Tsai and C Y Sue, "Review of MEMS-based drug delivery and dosing systems," *Sensors Actuators A* Vol. 134, pp. 555-564, 2007.
- [5] L Chen, S Lee, J Choo and E K Lee, "Continuous dynamic flow micropumps for microfluid manipulation," *J. Micromech. Microeng.* Vol. 18, pp. 1-22, 2008.
- [6] F Amirouche, Y Zhou and T Johnson, "Current micropump technologies and their biomedical applications," *Microsyst. Technol.* Vol. 15, pp. 647-666, 2009.
- [7] H Andersson, W van der Wijngaart, P Nilsson, P Enoksson and G Stemme, "A valve-less diffuser micropump for microfluidic analytical systems," *Sensors Actuators B* Vol. 72, pp. 259-265, 2001.
- [8] B Fan, G Song and F Hussain, "Simulation of a piezoelectrically actuated valveless micropump," *Smart Mater. Struct.* Vol. 14, pp. 400-405, 2005.
- [9] G H Feng and F S Kim, "Micropump based on PZT unimorph and one-way parylene valves," *J. Micromech. Microeng.* Vol. 14, pp. 429-35, 2004.
- [10] J Kang, J V Mantese and G W Auner, "A self-priming, high performance, check valve diaphragm micropump made from SOI wafers," *J. Micromech. Microeng.* Vol. 18, pp. 1-8, 2009.
- [11] R. Rapp, W K Schomburg, D. Maas, J. Schulz and W. Stark, "LIGA micropump for gases and liquids," *Sens. Actuators A* Vol. 40, pp. 57-61, 1994.
- [12] W K Schomburg, J. Fahrenberg, D. Maas, R. Rapp, "Active valves and pumps for microfluidics," *J. Micromechanics Microeng.* Vol. 3, pp. 216-218, 1993.
- [13] S Boehm, W Olthuis and P Bergveld, "A plastic micropump constructed with conventional techniques and materials," *Sensors Actuators A* Vol. 77, pp. 223-228, 1999.
- [14] S. Santra, P. Holloway, D. Batich, "Fabrication and testing of a magnetically actuated micropump," *Sens. Actuators B* Vol. 87, pp. 358-364, 2002.
- [15] T Q Truong and N T Nguyen, "A polymeric piezoelectric micropump based on lamination technology," *J. Micromech. Microeng.* Vol. 14, pp. 632-638, 2004.
- [16] J H Kim, K T Lau, R Shepherd, Y Wu, G Wallace and D Diamond, "Performance characteristics of a polypyrrole modified polydimethylsiloxane (PDMS) membrane based microfluidic pump," *Sensors and Actuators A* Vol. 148, pp. 239-244, 2008.

Chiang-Ho Cheng received his BS degree in systems and naval mechatronic engineering from National Cheng Kung University, Tainan, Taiwan, in 1986. He received MS and PhD degrees from the Institute of Applied Mechanics in National Taiwan University, Taiwan, in 1988 and 1993, respectively. He now is an distinguished professor at the Department of Mechanical and Automation Engineering of Da-Yeh University, Changhua, Taiwan. His present research interests concern piezoelectric actuators, including blade or sol-gel thick piezoelectric film and bulk piezoelectric ceramics, and their applications for MEMS, such as microdroplet ejectors, micromirrors, dispensers and micropumps.